Analytical Methods

PAPER

View Article Online
View Journal | View Issue

Cite this: *Anal. Methods*, 2014, **6**, 4421

Simultaneous extraction of anthracyclines from urine using water-compatible magnetic nanoparticles with a dummy template coupled with high performance liquid chromatography†

Wenyue Zou,‡[a] Pierre Dramou,‡[a] Lien Ai Pham-Huy,[b] Kai Zhang,[a] Jia He,[a] Chuong Pham-Huy,[c] Deli Xiao*[a] and Hua He*[ade]

Water-compatible magnetic molecularly imprinted polymers (M-MIPs) for extraction and pre-concentration of anthracyclines (ANTs) from urine have been successfully synthesized by a non-covalent method using epirubicin (EPI) as a dummy template, methacrylamide as a functional monomer, and ethylene glycol dimethacrylate as a cross-linker. The obtained M-MIPs were characterized by scanning electron microscopy (SEM), transmission electron microscopy (TEM), Fourier transform infrared spectroscopy (FT-IR), X-ray diffraction (XRD) and vibrating sample magnetometer (VSM). Adsorption kinetic and isotherm studies were carried out, which indicated that the M-MIPs displayed a rapid dynamic process and a high adsorption capacity. The adsorption behavior was discussed in detail, showing that it could be described as a chemisorption process and both external surface diffusion and intra-particle diffusion contributed to the adsorption mechanism. Furthermore, the binding sites were found to be heterogeneous for M-MIPs, while homogeneous for M-NIPs. The selectivity of M-MIPs demonstrated higher affinity for target EPI and EPI-analogues over other structurally unrelated compounds. A rapid solid-phase extraction (SPE) method using M-MIPs as sorbents coupled with high performance liquid chromatography (HPLC) was established for simultaneous determination of ANTs in urine samples. The recoveries ranged from 93.9% ± 5.2% to 100.0% ± 3.4% with the limit of detection of 0.6–2.4 ng mL^{-1}. Moreover, the M-MIPs could be regenerated, which could be utilized for several cycles with no obvious decrease in the adsorption capacity. The results indicated that the proposed method is a practical approach for simultaneous determination of ANTs in urine.

Received 26th January 2014
Accepted 9th April 2014

DOI: 10.1039/c4ay00232f

www.rsc.org/methods

1. Introduction

Anthracyclines (ANTs) are widely used as anticancer agents in the treatment of various forms of cancer. Notwithstanding the favorable therapeutic index, their cardiotoxicity is a serious problem. ANTs belong to cytostatic agents which act by either inhibiting cell growth or directly killing cells;[1] their clinical use has been compromised by a cumulative dose-dependent irreversible chronic cardiomyopathy. Therefore, monitoring the concentration and residues of these drugs in the urine of patients is of great significance to determine the correct patient intake. Various methods have been described for the determination of ANTs, including capillary electrophoresis,[2,3] resonance light scattering,[4] fluorometry[5] and HPLC with a different detector.[6–11] Even though some of these methods are sensitive, they require the use of some expensive instruments. HPLC coupled with ultraviolet detector (UVD) as a common apparatus in an analytical laboratory is the universal approach to the detection of various drugs. However, it is unsatisfactory for the quantitative determination of ANTs due to their extremely low concentration and the interference of the complex matrix in biological fluids. Therefore, enrichment and sample pretreatment processes are required. In order to overcome drawbacks such as time-consuming[12] and solvent-dependent[13] nature of the conventional pretreatment technique, it is necessary to develop a practicable approach with specific recognition and

[a]*Department of Analytical Chemistry, China Pharmaceutical University, 24 Tongjia Lane, Nanjing 210009, Jiangsu, China. E-mail: jcb315@163.com; dochehua@163.com (H. He); xiao49562000@163.com (D. Xiao); Fax: +86 025 83271505; Tel: +86 025 83271505*

[b]*Department of Pharmacy, Stanford University Medical Center, Palo Alto, CA, USA*

[c]*Faculty of Pharmacy, University of Paris V, 4 Avenue de l'Observatoire, 75006 Paris, France*

[d]*State Key Laboratory of Natural Medicines, China Pharmaceutical University, Nanjing 210009, China*

[e]*Key Laboratory of Drug Quality Control and Pharmacovigilance, China Pharmaceutical University, Ministry of Education, 24 Tongjia Lane, Nanjing 210009, Jiangsu, China*

† Electronic supplementary information (ESI) available: See DOI: 10.1039/c4ay00232f

‡ These authors contributed equally to this work and should be considered co-corresponding authors.

time-saving properties for the separation and enrichment of these important anticancer drugs.

Molecularly imprinted polymers (MIPs) as synthetic polymers with cavities, which are suitable for the target template molecule and similar compounds, have many advantages such as good recognition property, stability to extreme temperature and pH, flexibility and low cost. They were applied in the drug delivery system of ANTs in recent years.[14,15] Besides, MIPs have become increasingly attractive in the analytical field as SPE sorbents. The molecularly imprinted-SPE (MISPE) allows the analyte to be pre-concentrated while the interference compounds to be removed from the matrix simultaneously. This technique has been successfully applied in multiple domains[16–18] by now. However, the cartridge mode utilized in MISPE is an obstacle in its application due to the tedious column-packing procedure and high back-pressure. When magnetic components are encapsulated into MIPs, the synthesized products, M-MIPs, not only possess magnetic characteristic, but also have specific and selective recognition property to the template molecule. They are being considered as one of the most popular sorbents for pre-concentration methods of trace analysis.[19] Magnetic-MIPs in SPE can build a controllable extraction process and allow magnetic separation to replace the conventional time-consuming operation.[20] In the magnetic MISPE procedure, M-MIPs can be added into a solution or suspension containing target analytes, and then easily separated from the matrix *via* an external magnetic field, avoiding the process of making packed columns or the additional centrifugation and filtration as in traditional SPE.[21–23]

However, there is a general concern which relates to the poor level of recognition of the M-MIPs to the analyte in aqueous media. The majority of M-MIPs were synthesized in aprotic and low polar organic solvents. When applied in polar solvents such as water environment, the formation of the pre-polymerization complex during the imprinting procedure can be disturbed, and the hydrogen bonding interactions between template molecules and functional monomers can be destroyed, leading to a lower affinity between M-MIPs and the analyte.[24] Accordingly, application of MIPs in aqueous media is still a challenging and difficult task. In order to obtain MIPs that can selectively recognize the template in aqueous media, it is necessary to exploit other intermolecular interactions, such as ionic interactions,[25] to replace hydrogen bonding interactions. Another widely used approach is the hydrophilic modification on the surface of materials, such as grafting hydrophilic polymeric chains[26] or introducing hydrophilic monomers pre-polymerization.[27] Although a few studies about MISPE in aqueous environment were reported, they basically dealt with the separation and binding performance, and there was no detailed knowledge on the adsorption mechanism of MISPE in aqueous media for ANTs. Compared with these methodologies, we proposed a simple and time-saving solution by utilizing a high amount of oleic acid in the polymer synthesis process to make M-MIPs water compatible.[14] Furthermore, a detailed discussion about the adsorption mechanism was conducted.

In the present work, water-compatible M-MIPs with selective recognition property intended to extract and pre-concentrate ANTs from human urine were prepared. EPI was chosen as the dummy template to avoid the inherent bleeding of trace amount of EPI when detecting the other ANTs. EPI consists of an aglycone ring coupled to an amino sugar, representing the essential structural features of ANTs. The nature of the structure makes it a suitable dummy template in the recognition of other ANTs. In other words, any compounds with these exact structural features are expected to be recognized by the synthesized EPI-M-MIPs. To the best of our knowledge, it is the first attempt to use a dummy template to prepare M-MIPs as sorbents of SPE for the rapid recognition and simultaneous extraction of ANTs from aqueous media coupled with HPLC-UV analysis. The M-MIPs obtained were characterized by SEM, TEM, FT-IR, XRD and VSM methods. The equilibrium and kinetic data of the adsorption process were then analyzed in detail to study the adsorption kinetics and isotherms of EPI onto the M-MIPs. The ANTs recognition and separation from spiked urine samples were realized by using M-MIPs as SPE sorbents. Subsequently, by using methanol–acetic acid as the elution solution, the two ANTs were selectively extracted from urine samples and all matrix interferences were eliminated simultaneously with satisfactory recovery and high selectivity.

2. Experimental

2.1. Materials

Epirubicin, Doxorubicin (DOX) and Daunorubicin (DAUN) were purchased from Shandong New Time Pharmaceutical Co., Ltd, China. Gatifloxacin (GTFX) and ferric chloride hexahydrate $FeCl_3 \cdot 6H_2O$ (Fe^{3+}) were purchased from Sinopharm Chemical Reagent Co., Ltd. (Shanghai, China). Ferrous sulfate heptahydrate $FeSO_4 \cdot 7H_2O$ (Fe^{2+}) and dimethyl sulfoxide (DMSO) were purchased from Nanjing Chemical Reagent Co., Ltd (Nanjing, China). Methacrylamide (MAM), ethylene glycol dimethacrylate (EGDMA), polyvinylpyrrolidone (PVP), azobisisbutyronitrile (AIBN), and oleic acid were obtained from Aladdin Industrial Corporation (Shanghai, China). Sodium dihydrogen phosphate, $NaH_2PO_4 \cdot 2H_2O$, was purchased from Shanghai Lingfeng Chemical Reagent Co., Ltd (Shanghai, China) and the phosphoric acid was obtained from Nanjing Chemical Reagent Co., Ltd (Nanjing, China). All these chemicals and solutions used were of analytical reagent grade. Methanol and acetonitrile of HPLC grade were purchased from Jiangsu Hanbon Sci.&Tech. Co., Ltd (Huaian, China) and Nanjing Chemical Reagent Co., Ltd (Nanjing, China), respectively. Ultrapure water was prepared by using an ultrapurification system (Chengdu, China) and used throughout the experiments.

2.2. Instruments and HPLC analysis

To characterize the nanomaterials synthesized, an S-3000 scanning electron microscope (SEM, Hitachi Corporation, Japan) and a FEI Tecnai G2 F20 transmission electron microscope (TEM) were used to examine the size and the morphology of the nanomaterials. Their surface functional groups were measured with a 8400s FT-IR spectrometer purchased from Shimadzu (Kyoto, Japan). The X-ray powder diffraction pattern (XRD) was performed using an X′ TRA X-ray diffractometer with Cu Kα irradiation at $\gamma = 0.1541$ nm for phase identification. To

confirm the magnetic properties, tests were done using a LDJ 9600-1 vibrating sample magnetometer (VSM) operating at room temperature with applied fields up to 10 kOe.

The HPLC analysis system consisted of a quaternary pump G1311C, an auto liquid sampler (SLA) G1329B, a column thermostat G1316A and an ultraviolet detector G4212B. Chromatographic separations were carried out using a column purchased from Agilent Technologies (Waldbroun, Germany) (type Eclipse Plus C18, 3.5 μm, 4.6 mm × 100 mm), with the column temperature operated at 30 °C. The detection was at $\lambda = 254 \pm 2$ nm, reference $\lambda = 360 \pm 2$ nm. The data were acquired and processed by means of HP ChemStation for LC software. The mobile phase was a mixture of phosphate buffer (1%, pH 2.35)–methanol–acetonitrile (60 : 20 : 20, v/v/v). The injection volume was 10.0 μL, and the mobile phase flow rate was kept constant at 1.0 mL min^{-1}.

2.3. Synthesis of M-MIPs

The preparation of Fe_3O_4 was performed by a chemical co-precipitation of Fe^{2+} and Fe^{3+} ions following our previous report.[28] The experimental procedure was described in ESI Appendix S1.† Subsequently, the M-MIPs were prepared using the synthesized Fe_3O_4 magnetic nanoparticles. The mixture of EPI (1.0 mmol) and MAM (9.0 mmol) dissolved in DMSO (10.0 mL) was stirred for 0.5 h to prepare the preassembly solution. Fe_3O_4 (1.0 g) was mixed with DMSO (5.0 mL) under ultrasound for 10 min. Then EGDMA (20.0 mmol) and the preassembly solution were both added into the mixture of Fe_3O_4 in DMSO. This mixture was treated by ultrasound again for 0.5 h to prepare the pre-polymerization solution. PVP (0.4 g) was dissolved into 100 mL of DMSO–H_2O (9 : 1, v/v) in a three-necked round-bottomed flask. The mixture was stirred at 300 rpm and purged with nitrogen gas to displace oxygen at 60 °C. The pre-polymerization solution was then transferred into the flask followed by addition of AIBN (0.1 g). Two hours later, oleic acid (5.0 mL) was added to the flask. After reaction at 60 °C for 12 h, the polymers obtained were separated, and washed by interchanging water with the mixture of methanol–acetic acid (8 : 2, and 6 : 4, v/v) several times under ultrasound until EPI could not be detected by HPLC. Finally, the polymers collected were dried in a vacuum at 60 °C. The EPI-M-MIPs obtained could be used directly as sorbents for magnetic SPE. In parallel, the magnetic non-imprinted polymers (M-NIPs) were prepared in a similar way mentioned above and used as the control, but without adding EPI.

2.4. Adsorption kinetic study

In the adsorption kinetic experiment, 5.0 mg of M-MIPs or M-NIPs was mixed with 50.0 mL of EPI solution at a concentration of 10.0 μg mL^{-1} and incubated at room temperature for 3 h with shaking. After different time intervals (from 0 min to 180 min), the sorbent with captured EPI was separated from the suspension with a magnet and the supernatant was then analyzed by HPLC. According to the concentration of EPI before and after adsorption respectively, the amount of EPI bound to M-MIPs or M-NIPs was calculated following eqn (1):

$$Q = (C_0 - C_t)\frac{V}{m} \quad (1)$$

where C_0, C_t, V and m represent the concentration (μg mL^{-1}) of EPI in solution before and after the adsorption process, the volume of the solution (mL) and the weight of the polymer (mg), respectively. The average results from triplicate independent results were used for the following discussion.

2.5. Adsorption isotherm study

Static equilibrium adsorption tests were performed by suspending 4.0 mg of polymers (M-MIPs or M-NIPs) in 4.0 mL of EPI solution with different concentrations ranging from 5.0 μg mL^{-1} to 50.0 μg mL^{-1}. The screw-capped centrifuge tubes were used as batch reactor systems. All tubes were sealed and executed with ultrasonic-processing for 5 min. Then the mixture was kept for 2 h at room temperature with shaking. After that M-MIPs were separated by an external magnet. The concentration of free EPI in the supernatant was measured by HPLC analysis. The amount of EPI bound to M-MIPs or M-NIPs was calculated by eqn (1).

2.6. Selectivity study

A standard mixture solution of EPI, DOX, DAUN and GTFX with an initial concentration of 20.0 μg mL^{-1} was prepared. 4.0 mg of M-MIPs or M-NIPs was mixed with 4.0 mL of the mixture solution, respectively. The adsorption process was conducted as described earlier for the adsorption isotherm experiments.

2.7. Optimization of the SPE procedure

Conditions affecting the performance of the extraction, such as the amount of M-MIPs, the adsorption time and the elution solvent, were investigated to achieve high recovery for ANTs. The SPE procedure was optimized by analyzing spiked DOX and DAUN in urine samples (10.0 μg mL^{-1}). Different amounts of M-MIPs ranging from 0.5 to 4.0 mg, adsorption time from 10 to 90 min and a variety of elution solvents including water, methanol and methanol–acetic acid (9 : 1, 8 : 2, 6 : 4, v/v) were established. When one parameter was changed, the other ones were kept at their optimal values.

2.8. Determination of two ANTs in urine sample

For the selective recognition and extraction of ANTs from a urine sample, a 4.0 mL aliquot of urine from non-treated human sources spiked with DOX and DAUN at the final concentration of 0.1, 1.0 and 10.0 μg mL^{-1} was prepared and loaded onto 3.0 mg M-MIPs and M-NIPs, respectively. After incubation for 2 h at room temperature, M-MIPs and M-NIPs were removed by a permanent magnet and washed with 4.0 mL of water. Then 1.0 mL mixture of methanol–acetic acid (8 : 2, v/v) was used to elute ANTs adsorbed. The eluted solution was concentrated in a vacuum. After that, the residue was dissolved in 0.4 mL mobile phase. Finally, the treated samples were analyzed by HPLC.

2.9. Reusablilty of M-MIPs

The adsorption–desorption cycle was repeated 5 times by using the same imprinted material in order to show the reusability of the M-MIPs. The adsorption process was conducted as described earlier for the adsorption isotherm experiments. The desorption process was implemented as the washing procedure after the polymerization.

3. Results and discussion

3.1. Synthesis of M-MIPs

The synthetic approach comprised the following steps: (1) preparation of a Fe_3O_4 core; (2) self-assembly of the template molecule (EPI) and functional monomer (MAM); (3) polymerization of the pre-polymeric mixture on the surface of the Fe_3O_4 core in the presence of cross-linker (EGDMA), initiator (AIBN), dispersant agent (PVP), dispersing medium (DMSO) and a special additional agent (oleic acid); and (4) elution of template molecules (EPI) with a series of washing processes.

The self-assembling process between template molecule and functional monomer is a key step in the preparation of MIPs. High strength of the complex formed between the template and the monomer represents an essential condition to obtain polymers with good specificity and affinity. Hydrogen bonds, belonging to the non-covalent forces, play a leading role in the self-assembling process. MAM is a reliable functional monomer for EPI.[14] The amide group of MAM is the main part in the hydrogen bond formation because it can interact with both hydrogen bond receptor and donor of EPI. The nitrogen atom of MAM amide group can form a hydrogen bond with the hydrogen atom of EPI hydroxide group. Moreover, it is possible to donate two hydrogen atoms to form hydrogen bonds with oxygen atoms of EPI. This ability of MAM makes it possible to obtain heterogeneous binding sites of the EPI template on the imprinted polymer.

The oleic acid acts as an anionic surfactant which contains carboxylic groups and could provide a large amount of negatively charged functional groups on the surface of MIPs. These carboxylic groups and the positive metal ions such as ferric ions of the magnetic particles in the system would interact through electrostatic attraction. By this means the MIPs are grafted onto the magnetic particles. After the reaction with the carboxylic groups of oleic acid, there are hydrophobic carbon chains existing outside the template molecule-functional monomer polymer, which can prevent H_2O molecules from going inside to destroy the hydrogen bonds when the polymer is dissolved in aqueous media.

In order to acquire M-MIPs with high selective recognition and adsorption capacity, the synthesis conditions such as the polymerization time and temperature played important roles. According to our previous research,[29] the polymerization time and temperature were controlled at 12 h and 60 °C to obtain M-MIPs with appropriate thickness and particle size.

3.2. Characterization

The FT-IR spectra (Fig. S1†), XRD patterns (Fig. S2†) and their explanations reported in ESI Appendix S1 and S2† indicate the successful preparation of the M-MIPs or M-NIPs shells on the surface of iron oxide beads.

The SEM image in Fig. 1a at 300 nm and TEM image in Fig. 1b at 100 nm show the morphology features of the resulting materials. Some agglomerations can be observed in Fig. 1a and among them exist large cavities. The porosity plays a significant role in adsorption and elution processes by increasing the adsorption capacity when recognizing the analytes and improving the mass transfer rate when rebinding them. From Fig. 1b, it can be observed that the materials are uniform spheres with the size inferior to 500 nm.

Fig. 2a shows the hysteresis loops of the magnetite particles recorded at room temperature. The magnetic saturation (M_s) values are 51.62 and 10.17 emu g^{-1} for the Fe_3O_4 and M-MIPs, respectively. The decrease in the magnetization value from the pure iron oxide to M-MIPs can be attributed to the coating process around the Fe_3O_4; the magnetically inactive shell has shielded the magnetite. Compared with the values reported in other articles,[30,31] these M-MIPs can be considered to exhibit superior magnetic property. As shown in Fig. 2b, M-MIPs still remained strongly magnetic to meet the need of magnetic separation. It can be easily isolated from the aqueous solution within a few seconds by placing an external magnetic field near the glass bottle and the supernatant is colorless.

3.3. Adsorption kinetic study

The initial concentration of the EPI solution was 10.0 μg mL^{-1}. The adsorption time range was from 0 min to 180 min. Fig. 3 indicates the procedure of the adsorption kinetics of the EPI solution onto M-MIPs and M-NIPs. In the case of M-MIPs, the adsorption amount increased with the time in the first 50 min and then remained stable in the following time. Obviously, the adsorption amount of M-NIPs was smaller. In addition, with M-NIPs it was easier to reach equilibrium. It was less than 20 min for them to get the maximum adsorption amount. It means that there were imprinted cavities and specific binding sites existing inside the M-MIPs, which could recognize the template molecule and its analogues. In the first 50 min, they took up the cavities and sites gradually, resulting in the increasing of the adsorption amount. But for M-NIPs, there was no such imprinted cavity or specific binding site. EPI molecules were adsorbed on the surface of M-NIPs, and the binding site was limited. So the adsorption amount was low and the equilibrium was easy to attain.

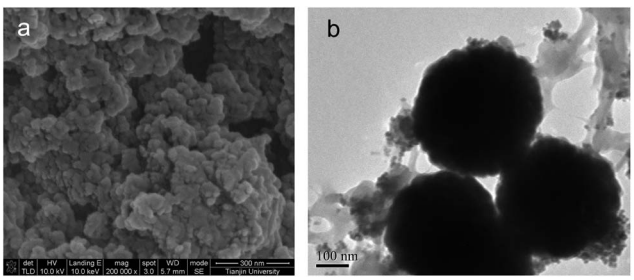

Fig. 1 SEM image (a) and TEM image (b) of M-MIPs. Scale bars: 300 nm for (a) and 100 nm for (b).

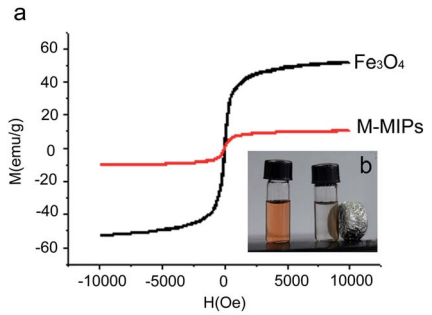

Fig. 2 Magnetization curves of Fe_3O_4 and M-MIPs (a) and the magnetic performance of M-MIPs within a few seconds using an external magnetic field (b).

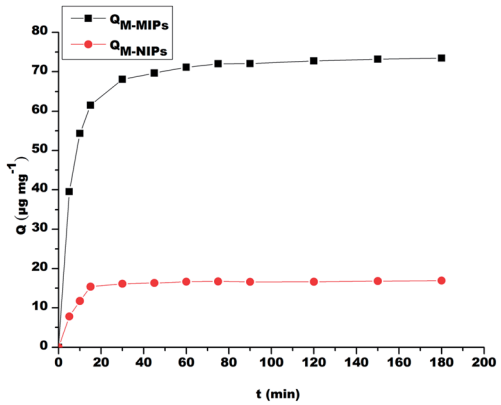

Fig. 3 Adsorption kinetic curves for EPI on M-MIPs and M-NIPs (EPI: initial concentration: 10.0 μg mL^{-1}, volume: 50.0 mL; M-MIPs or M-NIPs amount: 50.0 mg; adsorption time: 0 min to 180 min).

In our study, two different models: pseudo-first-order model and pseudo-second-order model were used for further analysis of the adsorption process, and the intra-particle diffusion model was used to examine the adsorption mechanism.

The pseudo-first-order model is described as:

$$\ln (Q_e - Q_t) = \ln Q_e - K_1 t \quad (2)$$

where Q_e and Q_t represent the amount (μg mg^{-1}) of EPI adsorbed at equilibrium and time t (min), respectively, and K_1 is the rate constant for pseudo-first-order model. A straight line from a plot of $(Q_e - Q_t)$ *versus* t should be obtained if the model is applicable.

The pseudo-second-order model is described as:

$$\frac{t}{Q_t} = \frac{t}{Q_e} + \frac{1}{K_2 Q_e^2} \quad (3)$$

where Q_e and Q_t refer to the amount (μg mg^{-1}) of EPI adsorbed at equilibrium and time t (min), respectively, and K_2 is the equilibrium rate constant for the pseudo-second-order model. The Q_e and K_2 values can be calculated from the slope and intercept of the linear plot of t/Q_t *versus* t, respectively.

The parameters calculated are listed in Table 1. A plot of t/Q_t *versus* t was obtained as a straight line with high correlation coefficient, which showed that the adsorption process of EPI followed the pseudo-second-order kinetic model. Furthermore, the amounts of drug adsorbed at equilibrium (Q_e) calculated according to the pseudo-second-order model were more in accordance with the experimental data, which also indicated that the adsorption of EPI onto M-MIPs could be better described by the pseudo-second-order model than the first one.

The initial adsorption rate (h_2, mg g^{-1} min^{-1}) was calculated according to the following equation:[32]

$$h_2 = K_2 Q_e^2 \quad (4)$$

The rate constant (K_2) depended on the surface coverage fraction of the drugs, which was a complex function of the initial concentration of the solution.[33] The h_2 values calculated were 5.16 and 21.32 for M-MIPs and M-NIPs, respectively, which was a verification of our former explanation that there was no imprinted cavity or specific binding site inside M-NIPs, and the adsorption was fast taking place only on the nonspecific imprinted site of the polymers.

Based on the higher correlation coefficient (R^2) values which approached unity and the lower relative error, the pseudo-second-order model was therefore the most suitable equation to describe the adsorption kinetics of EPI on the binding sites of M-MIPs. This suggested that the overall rate of the adsorption process was controlled by chemisorption.[34] Epirubicin molecules were strongly held onto the binding sites of M-MIPs by several hydrogen bonds. On account of the strength and specificity of the hydrogen bonds involved, the adsorption process was better described as chemisorption than as physisorption.[32]

The pseudo-second-order model considered that all the steps of adsorption such as external diffusion and internal diffusion were mixed together, which made it difficult to identify the diffusion procedure. In order to study the adsorption mechanism, the intra-particle diffusion model based on the theory proposed by Weber and Morris was applied.[32] The intra-particle diffusion model is explored by the following equation:

$$Q_t = K_i t^{0.5} + C_i \quad (5)$$

where Q_t is the amount (μg mg^{-1}) of EPI adsorbed at time t (min), K_i is the intra-particle diffusion rate constant (mg g^{-1} min^{-1}), which is obtained from the slope of the straight line of Q_t *versus* $t^{0.5}$. C_i is the intercept of the line, and represents the thickness of the boundary layer. A larger C_i means a greater effect of the boundary layer.[34] If the plot of Q_t *versus* $t^{0.5}$ is a single line which passes through the origin, then the intra-particle diffusion is the sole rate-limiting step. However, the data obtained from this study exhibited a multi-linear plot, indicating that some other steps were involved during the adsorption process. Regarding the adsorption on M-MIPs, the plot could be divided into three stages (Fig. 4): an initial sharp rise step was followed by a gradual increase stage and a final plateau. The first step represented the external boundary adsorption which is ascribed to the diffusion of EPI through the solution to the external surface of M-MIPs[35] and the fast uptake

Table 1 Adsorption kinetic constants of the pseudo-first-order model and pseudo-second-order model for M-MIPs and M-NIPs

		Pseudo-first-order kinetic model				Pseudo-second-order kinetic model			
Materials	$Q_{e,exp}$ (μg mg^{-1})	$Q_{e,cal}$ (μg mg^{-1})	K_1 (min)	R_1^2	Relative error (%)	$Q_{e,cal}$ (μg mg^{-1})	K_2 (g mg^{-1} min^{-1})	R_2^2	Relative error (%)
M-MIPs	73.45	26.12	0.0329	0.9133	64.44	75.19	0.0037	1	2.37
M-NIPs	16.92	3.06	0.0252	0.7332	81.91	17.24	0.0174	0.9995	1.89

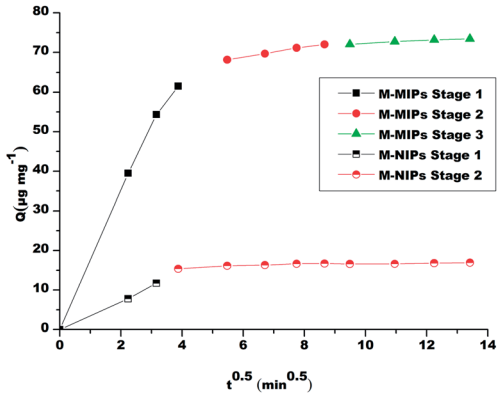

Fig. 4 Plot of the intra-particle diffusion model for adsorption of EPI on M-MIPs and M-NIPs (EPI: initial concentration: 10.0 μg mL^{-1}, volume: 50.0 mL; M-MIPs or M-NIPs amount: 50.0 mg; adsorption time: 0 min to 180 min).

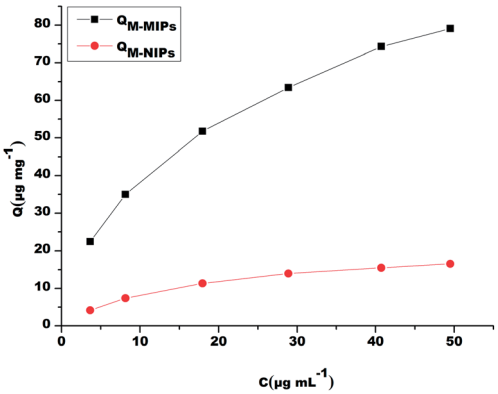

Fig. 5 Adsorption isotherm curves for EPI on M-MIPs and M-NIPs (EPI: concentration: 5.0–50.0 μg mL^{-1}, volume: 4.0 mL; M-MIPs or M-NIPs amount: 4.0 mg).

of the most available sites on the external surface of M-MIPs.[36] The second step, namely the gradual adsorption stage, is attributed to the intra-particle diffusion when EPI gets transferred from the solution to the interior of M-MIPs. The plateau phase corresponded to the final equilibrium state where the migration of EPI started to slow down owing to the low concentration of EPI left in the solution. The plot of M-NIPs was divided into two parts (Fig. 4): the initial rapid rise portion reflected the external surface adsorption while the plain represented the final equilibrium stage. In the overall adsorption process, the adsorption rate was fast in the initial phase and slowed down with time elapsing. Moreover, it can be seen in Fig. 4 that only the first parts of the plots passed through the origin, suggesting that the intra-particle diffusion may not be the sole rate limiting factor in the adsorption process, and both external surface diffusion and intra-particle diffusion contributed to the adsorption mechanism.[37]

3.4. Adsorption isotherm study

Static adsorption tests were performed on 4.0 mg M-MIPs or M-NIPs with different initial concentrations of the EPI solution. The adsorption isotherm plotted in Fig. 5 indicates that in the certain range of concentrations (5.0–50.0 μg mL^{-1}), the amount of EPI bound to M-MIPs and M-NIPs at adsorption equilibrium rose with the increase of initial concentration of EPI. In addition, the amount of EPI adsorbed by M-MIPs was higher than that by M-NIPs. Several adsorption models were employed to study the adsorption isotherm.[38]

The Langmuir isotherm model which assumes uniform adsorption on the surface of the sorbent was used to describe monolayer adsorption on a surface containing a finite number of binding sites with identical affinities.[35] The linear form of the equation is expressed as:

$$\frac{C_e}{Q_e} = \frac{C_e}{Q_m} + \frac{1}{Q_m K_L} \quad (6)$$

where C_e is the equilibrium concentration (μg mL^{-1}) of EPI in the bulk solution, Q_e is the equilibrium adsorption capacity (μg mg^{-1}), Q_m is the maximum adsorption capacity (μg mg^{-1}) which represents the total number of the binding sites, K_L is the Langmuir constant (mL μg^{-1}) related to the affinity of the binding sites.

The Langmuir isotherm equation can be expressed by a dimensionless constant called separation factor or equilibrium parameter R_L, which is defined as follows:

$$R_L = \frac{1}{1 + K_L C_0} \quad (7)$$

where C_0 is the initial concentration (μg mL^{-1}) of EPI. The parameter $R_L > 1$, $R_L = 1$, $0 < R_L < 1$, $R_L = 0$ indicates the isotherm shape according to unfavorable, linear, favorable and irreversible states, respectively.[39]

The Langmuir adsorption model is based on the assumption that the surface of the sorbent is relatively homogeneous. In contrast, the Freundlich model describes the adsorption on a heterogeneous surface which supports binding sites with varied affinities. The linear form of the isotherm equation is expressed as:

Table 2 Langmuir and Freundlich adsorption model parameters and correlation coefficient for EPI bound on M-MIPs and M-NIPs at 25 °C

	Langmuir adsorption model				Freundlich adsorption model		
Materials	Q_m (μg mg^{-1})	K_L (mL μg^{-1})	R_L	R^2	K_F (μg mg^{-1})	m	R^2
M-MIPs	89.29	0.14	0.60–0.95	0.9849	19.52	0.3797	0.9996
M-NIPs	21.10	0.07	0.22–0.80	0.9992	2.49	0.5082	0.9805

$$\log Q_e = m \log C_e + \log K_F \quad (8)$$

where K_F is an indicative constant (μg mg^{-1}) for adsorption capacity of the sorbent and m is known as the adsorption intensity or surface heterogeneity index. The value of m should be between 0 and 1, which when approaching 0 increases the heterogeneous character of the sorbent and when equal to 1 represents the homogeneous character.

The static adsorption data of EPI bound on M-MIPs and M-NIPs were analyzed by Langmuir and Freundlich models. The values of correlation coefficient (R^2) and the parameters obtained from the two models are summarized in Table 2.

The calculated R_L values were between 0 and 1, which indicated a favorable adsorption of EPI on M-MIPs and M-NIPs at the studied concentrations. The adsorption isotherm of EPI on M-MIPs was better fitted by the Freundlich adsorption model ($R^2 > 0.999$) while that on M-NIPs was more suited to the Langmuir adsorption model ($R^2 > 0.999$).

From another point of view, the Langmuir model is suitable for a homogeneous surface, while the Freundlich model is basically intended for a highly heterogeneous system, the system being more heterogeneous as the m value is closer to 0. The experimental data of M-MIPs ($m < 0.4$) proved the heterogeneity of the surface of M-MIPs. This was the consequence of the use of the high amount of functional monomer under non-covalent imprinting conditions, due to which the resulting M-MIPs contained a mixture of binding cavities of diverse affinities for the template molecule.[40] In parallel, the m value of M-NIPs ($m > 0.5$) suggested that although some degree of heterogeneity existed, a more homogeneous surface could be assumed.

In conclusion, M-MIPs had better applicability in the Freundlich adsorption model while M-NIPs had better applicability in the Langmuir model, indicating that M-MIPs contained heterogeneous binding sites and the surface of M-NIPs was homogeneous.

3.5. Selectivity study

Gatifloxacin was chosen as a reference compound to study the selectivity due to its different structure from ANTs. ESI Fig. S3† illustrates the adsorption capacity of M-MIPs and M-NIPs for these three structurally similar ANTs and the reference compound GTFX. It was obvious that the adsorption ability of M-MIPs was much higher than that of M-NIPs. In addition, the adsorption ability of the M-MIPs for these three ANTs was apparently higher than that of GTFX. Low adsorption capacity of M-MIPs for GTFX was observed because of the different structure compared with EPI. This result indicated that as to the substance which had significantly different structures from the template molecule, there was no specific site for it in the M-MIPs.[41]

To further investigate the adsorption ability of M-MIPs for different compounds under competitive conditions, the distribution coefficient (K_d), the selectivity coefficient (K) and relative selectivity coefficient (K') were calculated. The equations of these coefficients were interpreted in ESI Appendix S4.† The measured values are shown in Table 3.

The distribution coefficient K_d is a reflection of the adsorption capacity. A larger value of K_d suggests a stronger adsorption capacity of M-MIPs to the substance. The selectivity coefficient K represents the difference in the adsorption capacity of the same sorbent to different substances, while the relative selectivity coefficient K' represents the discrepancy between different sorbents. As can be seen in Table 3, M-MIPs had high discriminatory power between ANTs and the reference GTFX.

3.6. Optimization of the SPE procedure

The conditions of M-MIP amount, adsorption time and elution solvent were analyzed. As shown in ESI Fig. S4,† best recoveries were obtained when 3.0 mg of M-MIPs was added. ESI Fig. S5† indicates that 45 min was sufficient to achieve satisfactory recoveries. Further increase of the adsorption time did not

Table 3 The selectivity parameters of the M-MIPs and M-NIPs

	Distribution coefficient[a], K_d (mL mg^{-1})		Selectivity coefficient[b], K		
Analyte	M-MIPs	M-NIPs	M-MIPs	M-NIPs	Relative selectivity coefficient[c], K'
EPI	1.26	0.14	9.72	1.32	7.38
DOX	1.26	0.13	9.75	1.20	8.12
DAUN	1.72	0.20	13.31	1.85	7.18
GTFX	0.13	0.11			

[a] Distribution coefficient: $K_d = \frac{Q}{C_e}$. [b] Selectivity coefficient: $K = \frac{K_{d(ANTs)}}{K_{d(GTFX)}}$. [c] Relative selectivity coefficient: $K' = \frac{K_{M\text{-}MIPs}}{K_{M\text{-}NIPs}}$.

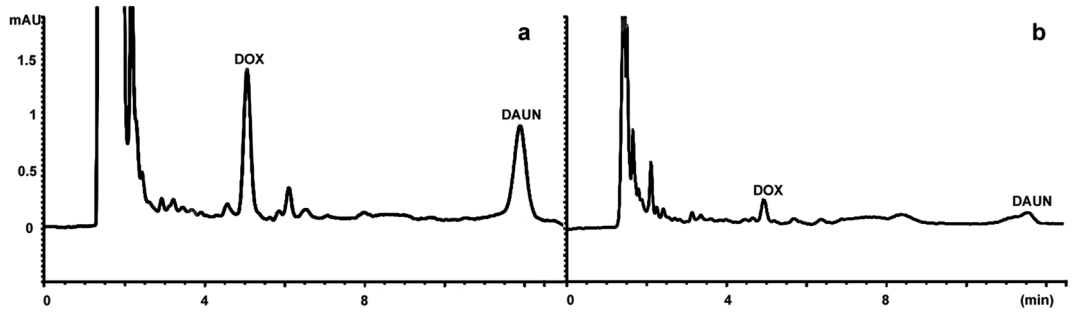

Fig. 6 Magnetic MISPE-HPLC chromatograms of DOX and DAUN (both 0.1 μg mL^{-1}) which were spiked in urine samples and extracted by EPI-M-MIPs (a) and EPI-M-NIPs (b) (urine samples: 4.0 mL, M-MIPs or M-NIPs amount: 3.0 mg).

Table 4 Determination of ANTs in urine samples using different methods

Method	Analytes	Linear range (μg mL^{-1})	LOD (ng mL^{-1})	Recovery (%)	RSD (%)	Reference
CZE-AD[a]	DAUN	1–100	400	93.2–109.0	≤4.7	3
DLR-fluorometry[b]	DOX	—	217	≥97	—	5
SPE-HPLC-MS/MS[c]	DOX, DAUN, EPI, IDA[e]	0.0001–0.002	0.01–0.04	79.1–102.0	≤9.1	11
M-MISPE-HPLC-UV[d]	DOX, DAUN	0.01–20.0	0.6–2.4	93.9–100.0	≤6.7	This work

[a] CZE-AD: capillary zone electrophoresis with amperometric detection. [b] DLR-fluorometry: dual lifetime referenced fluorometry. [c] SPE-HPLC-MS/MS: solid-phase extraction-high-performance liquid chromatography/tandem mass spectrometry. [d] M-MISPE-HPLC-UV: magnetic molecularly imprinted solid-phase extraction-high-performance liquid chromatography-ultraviolet detector. [e] IDA: Idarubicin.

result in improved recoveries. As can be seen in ESI Fig. S6,† using methanol–acetic acid (8 : 2, v/v) as the elution solvent was suitable and high recoveries were obtained.

3.7. Validation of the magnetic MISPE-HPLC method

The analytical performance of the magnetic MISPE-HPLC method was evaluated with a series of spiked urine samples. The linear range of the method was 0.01–20.0 μg mL^{-1}, with correlation coefficient 0.9991 for DOX and 0.9994 for DAUN. The LOD (limit of detection) and LOQ (limit of quantification) were obtained from the diluted samples and the signal-to-noise ratio (S/N). According to the experiment results, the LOD ($S/N = 3$) and LOQ ($S/N = 10$) were 0.6 ng mL^{-1} and 1.0 ng mL^{-1} for DOX, and 2.4 ng mL^{-1} and 5.0 ng mL^{-1} for DAUN, respectively. The enrichment factor was 10.

The precision of the method was investigated in terms of the intraday repeatability (the experiments were repeated 6 times) and interday reproducibility (6 different days) using 0.1, 1.0 and 10.0 μg mL^{-1} concentration levels for each analyte in the urine samples. The intraday repeatability was evaluated as the relative standard deviation (RSD) ranging from 0.3% to 3.2% and the interday reproducibility was less than 8% in all cases. The variations in the precision of the method might be due to the small amount of sample used.

3.8. Simultaneous determination of DOX and DAUN in urine samples

Urine samples spiked with different concentrations of DOX and DAUN (0.1, 1.0 and 10.0 μg mL^{-1}) were tested to evaluate the accuracy and applicability of the method. At each concentration, five independent measurements were implemented. The results are listed in ESI Table S1.† The calculated recoveries of DOX and DAUN in the urine samples ranged from 93.9% ± 5.2% to 100.0% ± 3.4%. As shown in Fig. 6, M-MIPs (Fig. 6a) performed much better than M-NIPs (Fig. 6b) when extracting DOX and DAUN from spiked urine samples. The results indicated the practical applicability of the method in this study for the simultaneous extraction and determination of ANTs from urine samples. Table 4 summarizes the performance of this method and other techniques reported in the literature,[3,5,11] respectively. Compared with the other methods, the simple method we proposed displays high sensitivity, low detection limits, appropriate linear range and satisfactory recovery without the use of expensive instruments.

3.9. Reusability of M-MIPs

The character of reusability is one of the outstanding advantages of M-MIPs, which makes the material an economical sorbent for SPE. Five adsorption–desorption cycles were performed in this study to investigate the regeneration of M-MIPs. The relative recovery fluctuated from 90.8% to 97.6%, which indicated that there was no significant loss in adsorption capacity. The properties of M-MIPs obtained in this study were stable in the bio-matrix samples.

4. Conclusion

In this study, M-MIPs using EPI as a dummy template were prepared by imprinting on the surface of Fe_3O_4 nanoparticles for simultaneous extraction and pre-concentration of ANTs

from urine. The proposed method overcame the problems of the traditional methods, such as the potential risk of residual template leakage, packing of the SPE column and the tedious centrifugation and filtration, thus ensuring the reliability and simplifying the sample pretreatment process. The adsorption mechanism of the synthesized polymers was investigated in detail for the first time. The research of selectivity showed that compounds with a structure identical to the template could be recognized and extracted simultaneously, which saved much time and cost of multiple sample pretreatment. The successful application in the simultaneous enrichment and determination of ANTs in urine samples indicated that the water-compatible M-MIPs coupled to the HPLC could be a promising tool in the analysis of these therapeutic agents in biological fluids.

Acknowledgements

This work was supported by Guizhou Provincial Natural Science Foundation of China (Grant no. 20122288), the Graduate Students Innovative Projects of Jiangsu Province (Program no. CXZZ11_0812) and by the National Basic Science Personal Training Fund (no. J0630858). The authors are delighted to acknowledge discussions with colleagues in their research group.

References

1 S. N. Mahnik, B. Rizovski, M. Fuerhacker and R. M. Mader, *Chemosphere*, 2006, **65**, 1419–1425.
2 H. Lu, G. Yuan, Q. He and H. Chen, *Microchem. J.*, 2009, **92**, 170–173.
3 Q. Hu, L. Zhang, T. Zhou and Y. Fang, *Anal. Chim. Acta*, 2000, **416**, 15–19.
4 Z. Chen, S. Qian, G. Liu, X. Chen and J. Chen, *Microchim. Acta*, 2011, **175**, 217–223.
5 F. Martínez Ferreras, O. S. Wolfbeis and H. H. Gorris, *Anal. Chim. Acta*, 2012, **729**, 62–66.
6 M. Pieri, L. Castiglia, P. Basilicata, N. Sannolo, A. Acampora and N. Miraglia, *Ann. Occup. Hyg.*, 2010, **54**, 368–376.
7 K. E. Maudens, C. P. Stove, V. F. J. Cocquyt, H. Denys and W. E. Lambert, *J. Chromatogr. B: Anal. Technol. Biomed. Life Sci.*, 2009, **877**, 3907–3915.
8 S. Ahmed, N. Kishikawa, K. Ohyama, M. Wada, K. Nakashima and N. Kuroda, *Talanta*, 2009, **78**, 94–100.
9 S. Nussbaumer, L. Geiser, F. Sadeghipour, D. Hochstrasser, P. Bonnabry, J.-L. Veuthey and S. Fleury-Souverain, *Anal. Bioanal. Chem.*, 2011, **402**, 2499–2509.
10 C. Sottani, P. Rinaldi, E. Leoni, G. Poggi, C. Teragni, A. Delmonte and C. Minoia, *Rapid Commun. Mass Spectrom.*, 2008, **22**, 2645–2659.
11 C. Sottani, G. Tranfo, M. Bettinelli, P. Faranda, M. Spagnoli and C. Minoia, *Rapid Commun. Mass Spectrom.*, 2005, **18**, 2426–2436.
12 T. Hu, Q. Le, Z. Wu and W. Wu, *J. Pharm. Biomed. Anal.*, 2007, **43**, 263–269.
13 A. L. Sanson, S. C. R. Silva, M. C. G. Martins, A. Giusti-Paiva, P. P. Maia and I. Martins, *Braz. J. Pharm. Sci.*, 2011, **47**, 363–371.
14 P. Dramou, P. Zuo, H. He, L. A. Pham-Huy, W. Zou, D. Xiao, C. Pham-Huy and T. Ndorbor, *J. Mater. Chem. B*, 2013, **1**, 4099–4109.
15 Q. Zhang, L. Zhang, P. Wang and S. Du, *J. Pharmaceut. Sci.*, 2014, **103**, 643–651.
16 F. F. Chen, R. Wang and Y. P. Shi, *Talanta*, 2012, **89**, 505–512.
17 N. Li, T. B. Ng, J. H. Wong, J. X. Qiao, Y. N. Zhang, R. Zhou, R. R. Chen and F. Liu, *Food Chem.*, 2013, **139**, 1161–1167.
18 L. Mergola, S. Scorrano, R. Del Sole, M. R. Lazzoi and G. Vasapollo, *Biosens. Bioelectron.*, 2013, **40**, 336–341.
19 Z. Zhang, W. Tan, Y. Hu, G. Li and S. Zan, *Analyst*, 2012, **137**, 968–977.
20 Y. Zhang, R. Liu, Y. Hu and G. Li, *Anal. Chem.*, 2009, **81**, 967–976.
21 M. Bouri, M. J. Lerma-García, R. Salghi, M. Zougagh and A. Ríos, *Talanta*, 2012, **99**, 897–903.
22 J. Zhan, G. Fang, Z. Yan, M. Pan, C. Liu and S. Wang, *Anal. Bioanal. Chem.*, 2013, **405**, 6353–6363.
23 D. Xiao, P. Dramou, N. Xiong, H. He, D. Yuan, H. Dai, H. Li, X. He, J. Peng and N. Li, *Analyst*, 2013, **138**, 3287–3296.
24 H. Yan, K. H. Row and G. Yang, *Talanta*, 2008, **75**, 227–232.
25 G. Qu, S. Zheng, Y. Liu, W. Xie, A. Wu and D. Zhang, *J. Chrom. B*, 2009, **877**, 3187–3193.
26 M. Singh, A. Kumar and N. Tarannum, *Anal. Bioanal. Chem.*, 2013, **405**, 4245–4252.
27 K. Hua, L. Zhang, Z. Zhang, Y. Guo and T. Guo, *Acta Biomater.*, 2011, **7**, 3086–3093.
28 P. Dramou, D. Xiao, H. He, T. Liu and W. Zou, *J. Sep. Sci.*, 2013, **36**, 898–906.
29 D. Xiao, P. Dramou, N. Xiong, H. He, H. Li, D. Yuan and H. Dai, *J. Chromatogr. A*, 2013, **1274**, 44–53.
30 X. Wang, H. Mao, W. Huang, W. Guan, X. Zou, J. Pan and Y. Yan, *Chem. Eng. J.*, 2011, **178**, 85–92.
31 W. Guo, W. Hu, J. Pan, H. Zhou, W. Guan, X. Wang, J. Dai and L. Xu, *Chem. Eng. J.*, 2011, **171**, 603–611.
32 M. C. Cela-Perez, M. M. Castro-Lopez, A. Lasagabaster-Latorre, J. M. Lopez-Vilarino, M. V. Gonzalez-Rodriguez and L. F. Barral-Losada, *Anal. Chim. Acta*, 2011, **706**, 275–284.
33 S. Azizian, *J. Colloid Interface Sci.*, 2004, **276**, 47–52.
34 I. A. W. Tan, A. L. Ahmad and B. H. Hameed, *J. Hazard. Mater.*, 2009, **164**, 473–482.
35 J. Pan, X. Zou, X. Wang, W. Guan, Y. Yan and J. Han, *Chem. Eng. J.*, 2010, **162**, 910–918.
36 M. Lopez Mdel, M. C. Perez, M. S. Garcia, J. M. Vilarino, M. V. Rodriguez and L. F. Losada, *Anal. Chim. Acta*, 2012, **721**, 68–78.
37 W. Liu, J. Zhang, C. Zhang, Y. Wang and Y. Li, *Chem. Eng. J.*, 2010, **162**, 677–684.
38 J. A. García-Calzón and M. E. Díaz-García, *Sens. Actuators, B*, 2007, **123**, 1180–1194.
39 T. Y. Guo, Y. Q. Xia, G. J. Hao, M. D. Song and B. H. Zhang, *Biomaterials*, 2004, **25**, 5905–5912.
40 R. J. Umpleby II, S. C. Baxter, M. Bode, J. K. Berch Jr, R. N. Shah and K. D. Shimizu, *Anal. Chim. Acta*, 2001, **435**, 35–42.
41 F. F. Chen, X. Y. Xie and Y. P. Shi, *J. Chromatogr. A*, 2013, **1300**, 112–118.